Expression of tyrosinase-like protein genes and their functional analysis in melanin synthesis of Pacific oyster (*Crassostrea gigas*)

Yijing Zhu [a], Qi Li [a,b,*], Hong Yu [a], Shikai Liu [a], Lingfeng Kong [a]

[a] *Key Laboratory of Mariculture, Ministry of Education, Ocean University of China, Qingdao 266003, China*
[b] *Laboratory for Marine Fisheries Science and Food Production Processes, Qingdao National Laboratory for Marine Science and Technology, Qingdao 266237, China*

ARTICLE INFO

ABSTRACT

Color polymorphism in Mollusca is of great interest for consumer preference. Although the heritability of shell color variation has been conducted by experimental crossing, little is known about molecular basis involved in these patterns. Tyrosinase-like proteins are important enzymes which are members of the type-3 copper protein superfamily. In this research, two tyrosinase-like protein genes including *CgTyp-1* and *CgTyp-3* were identified in the Pacific oyster *Crassostrea gigas*. Tissue expression analysis showed that *CgTyp-1* and *CgTyp-3* were dominantly expressed in the mantle. Particularly, they were expressed significantly higher in the edge mantle than that in the central mantle whether on the left or right mantles. Additionally, expressions of *CgTyp-1* and *CgTyp-3* were mainly found in the black shell color oysters, with relative lower levels in the white shell color oysters. In situ hybridization showed that positive signals for *CgTyp-1* and *CgTyp-3* were both detected within the outer epithelium of the outer fold either in the black or white shell color oysters. After interference, the expression levels of *CgTyp-1* and *CgTyp-3* mRNA were significantly attenuated, and the efficiency of RNAi reached 84.72% and 71.58%, respectively. Besides, knockdown *CgTyp-1* or *CgTyp-3*, obviously decreased the tyrosinase activity of mantles. Furthermore, the number of the melanosomes within epithelium of the outer fold was sharply reduced by silencing of each *Typ*. These findings argue that *CgTyp-1* and *CgTyp-3* may be involved in the melanin synthesis, which lends insight into regulation mechanism of shell pigmentation in *C. gigas*.

1. Introduction

Mollusks have high phenotypic variation and conspicuous coloration, and color patterns have attracted increasing interest from many different perspectives. Molluscan shellfish, as a major product of aquaculture, their shell color also influences consumers' preference (Alfnes et al., 2006). Although it has been demonstrated that shell color is influenced by environmental factors, such as substrate (Whiteley et al., 1997), temperature (Lecompte et al., 1998), salinity (Sokolova and Berger, 2000) or nutrition (Zhu et al., 2018), breeding studies have shown that shell color polymorphism is considered as a heritable trait, in some cases, which is controlled by variation at a single locus (Liu et al. 2009; Kobayashi et al. 2004). A large number of studies have been carried out to elucidate the molecular basis involved in shell pigmentation in molluscan shellfish (Aguilera et al., 2014; Jiang et al., 2020; Yao et al., 2020). However, the molecular processes that underlie the regulation of shell pigmentation in mollusks are not well understood.

Shell color is most commonly attributable to the presence of biological pigments (Williams, 2017). Chemical studies showed that molluscan shell pigments are composed of three of the more common classes of pigments identified to date, including melanins, porphyrins and carotenoids (Williams, 2017; Cai et al., 2011; Bergamonti et al., 2013). Melanin, as the most widespread pigment in nature, has been determined in many molluscan shellfish, such as cephalopods, gastropods and bivalves (Lemer et al., 2015). Melanin synthesis is a complex pathway in vertebrates (Hoekstra, 2006), within Mollusca it is best understood, although still incompletely in cephalopods (Derby, 2014). Melanosome is an unique organelle within which melanin pigments are synthesized and stored (Marks and Seabra, 2001). Multiple melanogenic enzymes and structural proteins act on the maturation of melanosomes (Palumbo, 2003). Tyrosinase (*Tyr*) is considered as melanosome-specific protein in this melanogenesis pathway (Hoekstra, 2006; Derby, 2014).

Tyrosinase and tyrosinase-like proteins (*Typs*) are important enzymes which are members of the type-3 copper protein superfamily

(Johansson and Soderhall, 1996). Interestingly, *Tyr* and *Typs* genes have been identified that they contribute to the shell pigmentation in mollusks, although in most studies it is not possible to rule out that these genes might function in the shell formation (Nagai et al., 2007; Chen and Chan, 2012; Feng et al., 2019; Zhu et al., 2021). In addition, *Tyr* expression and spatial localization in the organ responsible for shell pigmentation, the mantle, is consistent with a role in shell formation (Nagai et al., 2007). A study on *Pinctada fucata* showed that two tyrosinase proteins (*Pfty1* and *Pfty2*) were identified in the prismatic shell layer, specifing the role of tyrosinase genes in the shell melanin synthesis (Nagai et al., 2007). Jiang et al (2020) suggested that there might be a link between the shell formation and shell color by studying the expression of the *Rptyr9* gene in *Ruditapes philippinarum.* However, OT47 gene (a homolog of tyrosinase related protein 1) from *Pinctada margaritifera* associated with melanin synthesis was high expressed in the full albino strains compared with black and half albino strains, suggesting OT47 might over-express in order to overcompensate for a nonfunctional melanin protein in the full albino strains (Lemer et al., 2015).

The Pacific oyster (*Crassostrea gigas*), as an important bivalve species with economic value, has large production in the world. *C. gigas* displays a different shell color which is regarded as a quantitative trait, according to its continuous variation from near-white to near-black shells (Brake et al., 2004). Shell color has been viewed as a trait for increasing the commercial value of oysters (Nell, 2001), and thus is becoming new high potential traits. Up to now, more evidences are found that tyrosinase gene control the mantle edge pigmentation. In previous study, 26 tyrosinase genes were found from *C. gigas* genome (Feng et al., 2017). Knockdown tyrosinase by dsRNA interference blocked the shell growth in the *C. gigas*, confirming this gene was involved in the shell biomineralization (Feng et al., 2019). Comparison of black and white shell color *C. gigas* is an ideal method to identify the gene expression directly linked to shell pigmentation. Previously, we described their relationship, for which *Tyr* might play key role in the shell color pigmentation, while *Typ-2* might contribute to the shell formation and pigmentation (Zhu et al., 2021). However, functional studies about whether *Typs* regulate the melanin biosynthesis in *C. gigas* remains unclear.

RNA interference (RNAi) can induce post-transcriptional gene silencing in organisms to analyze the genes function in mammal (Cullen and Arndt, 2005) and insects (Boutros et al., 2004). In this research, two tyrosinase-like protein genes including tyrosinase-like protein 1 (*CgTyp-1*) LOC_105346503 and tyrosinase-like protein 3 (*CgTyp-3*) LOC_105348943 were identified in the *C. gigas* genome by a multi-omics data mining. Expression patterns of two genes were assessed in the black and white shell color oysters, which investigated the potential participation of *Typs* in the regulation of melanin synthesis. In particular, the exact effect of tyrosinase-like protein genes was deliberated by RNAi technology. These data enrich the knowledge of mechanisms of gene regulation in synthesis of melanin, which aid elucidation of their function in the shell color formation in the Pacific oyster.

2. Materials and methods

2.1. Phylogenetic analysis and gene structure prediction.

The amino acid sequences of tyrosinase/tyrosinase-like protein were retrieved from the NCBI database. Multiple alignment of the domains was conducted with the DNAMAN (Lynnon BioSoft), and signal peptide of *Typs* was predicted by Signal 4.1 (http://www.cbs.dtu. dk/services/SignalP/). For oyster *Typs* conserved domains, they were predicted by the online tool (SMART, http://smart.emblheidelberg.de/) (Letunic et al., 2015). Phylogenetic tree was constructed with MEGA 11.0 using neighbor-joining (NJ) method and 2000 bootstrap replicates. The detailed information of these sequences with their GeneBank accession numbers are as follows: *Mus musculus* tyrosinase isoform 2 (NP_001304326.1), *Xenopus laevis* tyrosinase-like (XP_041438658.1), *Danio rerio* tyrosinase (NP_571088.3), *Illex argentinus* tyrosinase 2

(BAC87844.1), *Sepia officinalis* tyrosinase (CAC82191.1), *Hyriopsis cumingii* Tyrosinase (APC92581.1), *Meretrix meretrix* tyrosinase (ALG64484.1), *Mizuhopecten yessoensis* tyrosinase-like protein 2 (XP_021373699.1), *Azumapecten farreri* tyrosinase (ACF25906.1), *P. margaritifera* tyrosinase 1 (CCE46151.1), *Pinctada imbricata* tyrosinase-like protein tyr-1 (AGR88240.1), *P. fucata* tyrosinase (AAZ66340.1), *P. fucata* tyrosinase-like protein (BAF74507.1), *Crassostrea virginica* tyrosinase-like protein 1 (XP_022344830.1), *C. gigas* tyrosinase-like protein 1 (XP_011453423.2), *C. gigas* tyrosinase-like protein 3 (XP_019918154.2).

2.2. Animals and sampling

Black and white shell oysters used for real-time PCR (qPCR) and in situ hybridisation (ISH) were supplied by the oyster farm in Weihai, Shandong, China (Fig. 1A), and were acclimated in artificial seawater for 1 week before processing. Tissue samples including anterior and posterior sides of the marginal mantles and central mantles of the both left and right sides (Aeml, Peml, Cml, Aemr, Pemr, Cmr; Fig. 1B), hemolymph, gill, adductor muscle, labial palps, and gonad were taken for immediate RNA extraction. Left mantles were obtained for ISH, and they were fixed in 4% paraformaldehyde in PBS for 12 h at 4 °C, then dehydrated, and stored at −20 °C in methanol until use.

2.3. RNA extraction and reverse transcription

Total RNA from various tissues were extracted following TRIzol protocol (Invitrogen). RNA concentrations, integrity, and quality were detected by NanoDrop 2000 (Thermo Scientific) and electrophoresis on 1% agarose gels. Total RNA (1000 ng) was converted to cDNA using the
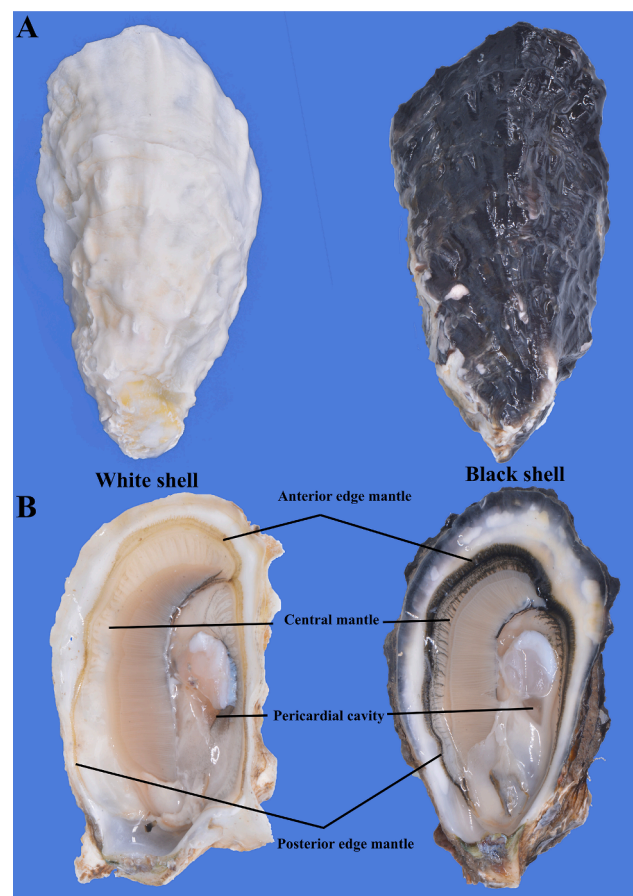

Fig. 1. The shell color (A) and different mantle regions (B) of *C. gigas*.

PrimeScriptTM reverse transcription kit (Takara).

2.4. Real-time PCR

Forward and reverse primers for qPCR were designed with Primer Premier 5, and as an internal control EF1α (Xu et al., 2018) were listed in Table 1. The reaction was run in a 10 μL volume using EvaGreen 2 × qPCR MasterMix-ROX (ABM) and was cycled 40 cycles at 95 °C for 5 s, 60 °C for 20 s, 72 °C for 20 s on a LightCycler® 480 machine (Roche, Switzerland). $2^{-\Delta\Delta CT}$ was used to calculate the relative quantification of target genes ($n = 9$).

2.5. In situ hybridization

Probes were synthesized in vitro using DIG RNA labeling Kit (Roche). To guarantee the authenticity of ISH experiment, negative controls (sense probe of *CgTyp-1*) were set up. Sense and antisense probes were tagged with a T7 promoter in forward and reverse primers respectively. The fixed mantles were dehydrated though a graded series of EtOH and cleared in xylene before transferring into paraffin. Then blocks were cut at 5 μm using a Leica RM 2016 microtome (Leica). After that, sections were de-waxed and treated with proteinase K (10 μg/mL, 10 min, 37 °C) before prehybridization (4 h, 60 °C). Sections were then conducted in hybridization buffer with sense or antisense probes at 60 °C for 16 h. Following this, sections were performed with anti-digoxigenin antibody (1 : 5000; Roche) in blocking buffer for 1 h at room temperature (RT), and then overnight at 4 °C. Color development was carried out in the NBT–BCIP mix (Roche). Sections were washed in ultrapure water, counterstained with 0.5% eosin, and digital images were captured using Olympus BX53 microscope.

2.6. RNAi experiment

Three-month-old black shell *C. gigas* (shell height: 58.13 ± 5.89 mm; shell length: 37.08 ± 4.47 mm) cultured in Weihai was selected for RNAi. Oysters were fed *Chlorella vulgaris*, and the water temperature was maintained at an average of 17 ± 1 °C for 1 week prior to processing. After the acclimation period, oysters were divided into the pre-experimental and experimental groups.

Small interference RNA (siRNA) for certain genes were synthesized by GenePharma (Shanghai, China) (Table 1). Oysters were anesthetized according to Liu et al (2019). The siRNA was diluted using 0.1 M PBS contained phenol red (1 : 20 diluted with DEPC). For RNAi experiment, 30 μL PBS containing 15 μg of siRNA was injected into the pericardial cavity of *C. gigas* (Fig. 1B), while the control group was injected with an equal volume of PBS also contained phenol red. In the pre-experiment, nine individuals were used in each treatment group (siRNA group and control group), then mantles were collected at 12, 24, 36 and 48 h post-injection by dissecting oysters using the sterilized scissors. Three individuals were set as biological replicates in each group. The expression levels of *CgTyp-1* and *CgTyp-3* performed by qPCR after injecting were used to identify the most efficient interference time for further experiment. In the experimental group, individuals were also divided into two groups, including siRNA group ($n = 45$) and control group ($n = 45$), then oysters were injected with the same dose of siRNA or PBS at 48-h-long interval at 1st, 3d, and 5th day. At the 7th day, mantles were obtained and frozen in liquid nitrogen until used for qPCR and tyrosinase activity assay. Meanwhile, mantles were fixed in 2.5% glutaraldehyde for electron microscopy.

2.7. Tyrosinase activity assays

Tyrosinase activity assay kit (Solarbio) was used to detect the tyrosinase activity of mantles. Briefly, 0.5 g mantle was homogenized with the lysis buffer under the ice water conditions. The solution was centrifugated to obtain the supernate, then supernate was mixed with buffer. After that, the mixture was incubated at 25 °C for 50 min, and tyrosinase activity was determined spectrophotometrically at 475 nm. Every set contained five oysters as biological replicates, tyrosinase activity was expressed as nmol/g wet weight.

2.8. Electron microscopy of mantles

Mantles were dehydrated through a graded acetone series, then postfixed in osmium tetroxide before embedding in EPON 812 resin. Then sections cut at 5 μm and then stained with toluidine blue for localization of different mantle regions under the light microscope. Ultra-thin sections of 60 nm were stained with uranyl acetate and lead citrate and observed by a transmission electron microscope (JEM-1200EX) at 80.0 kV.

2.9. Statistical analysis

Statistical analyses were conducted using SPSS 21.0 software. The comparison among samples was analyzed by One-way ANOVA test. Significant difference was indicated at $P < 0.05$ and $P < 0.01$.

3. Results

3.1. Sequence analysis of CgTyp-1 and CgTyp-3 in C. gigas

Amino acid sequences of *CgTyp-1* and *CgTyp-3* from *C. gigas* were aligned with the sequences from other bivalves (Fig. 2A). Sequence analysis of *CgTyp-1* showed 37.33% identity to P. margaritifera

Table 1
List of primers sequences used in this study.

| Primer names	Primer sequences (5′-3′)	Experiment
CgTyp-1-F	AAACAGACCTATGGACCTTTACGA	qPCR
CgTyp-1-R	GTTGGTAGCACAGGAAGGCATA	qPCR
CgTyp-3-F	GTAAGGACAGGTTTCTGTGGCAA	qPCR
CgTyp-3-R	GGCATCTCGTCTGGGTAATCG	qPCR
EF1α-F	AGTCACCAAGGCTGCACAGAAAG	qPCR
EF1α-R	TCCGACGTATTTCTTTGCGATGT	qPCR
CgTyp-1-F	GATCACTAATACGACTCACTATAGGGGGAACGGTCCAGTCGTCAAT	ISH
CgTyp-1-R	AGTTGGTAGCACAGGAAGGC	ISH
CgTyp-1-F	GGAACGGTCCAGTCGTCAAT	ISH
CgTyp-1-R	GATCACTAATACGACTCACTATAGGGAGTTGGTAGCACAGGAAGGC	ISH
CgTyp-3-F	GACGCCCCAAAATACTCCCA	ISH
CgTyp-3-R	GATCACTAATACGACTCACTATAGGGAGAGCTTCAGCATGGCTCTG	ISH
CgTyp-1-F	GCACCAAAUAACCCAAUAATT	siRNA
CgTyp-1-R	UUAUUGGGUUAUUUGGUGCTT	siRNA
CgTyp-3-F	CGGCAAACGUAGUGCAAAUTT	siRNA
CgTyp-3-R	AUUUGCACUACGUUUGCCGTT	siRNA
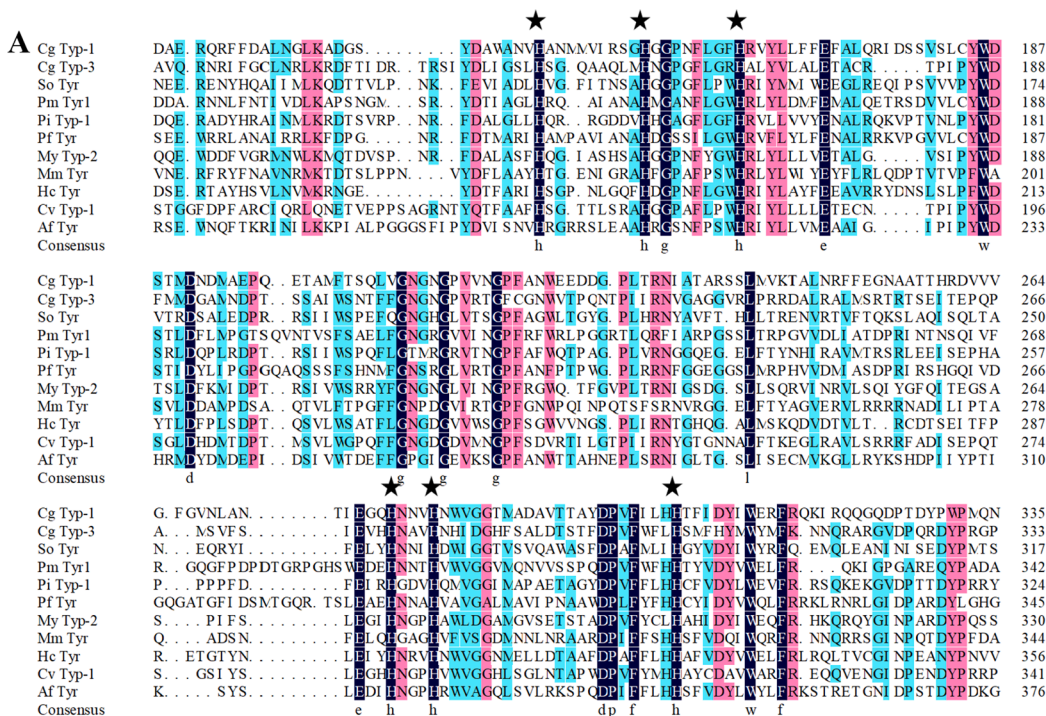
Fig. 2. Sequence alignment and phylogenetic analysis. A: Multiple sequence alignment of *CgTyp-1* and *CgTyp-3* with copper-binding domain from Molluscan. Conserved histidine residues are marked by ★. B: Schemes depicting the structure of *CgTyp-1* and *CgTyp-3* protein in *C. gigas*. The Cu (A) / Cu (B) domain with six conserved histidine residues is shown in green box. Blue box indicates trans-membrane region. Pink box indicates low complexity. C: Phylogenetic analyses of *Typs* genes.
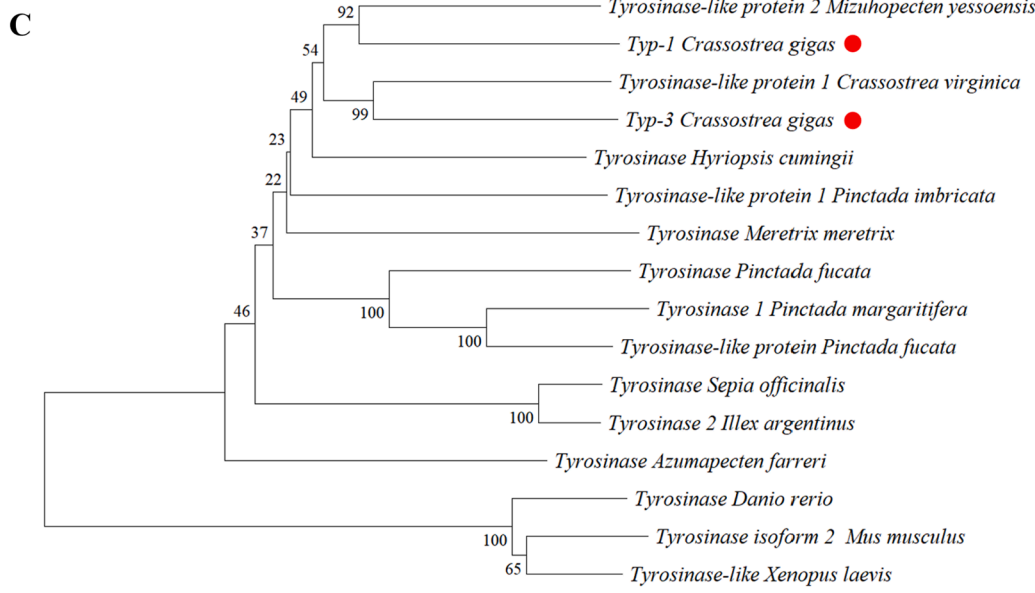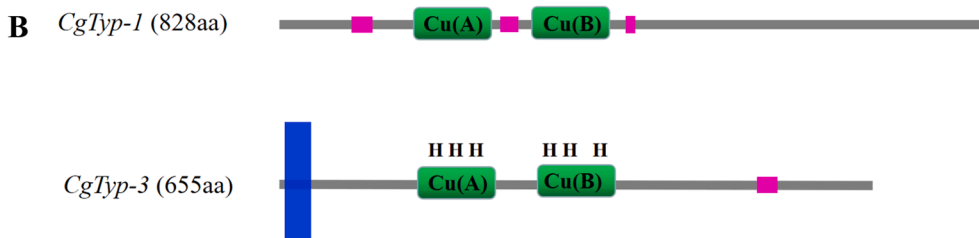
tyrosinase 1, 35.10% with tyrosinase of P. fucata, and 27.55% – 34.71% to other tyrosinase or tyrosinase-like proteins. The *CgTyp-3* showed 32.90% identity to P. imbricata tyrosinase-like protein 1, and 27.60% – 32.45% to other tyrosinase or tyrosinase-like proteins. It was notable that the *CgTyp-1* and *CgTyp-3* possessed six histidine residues, which was consistent with the observation in other species (Fig. 2A). In addition, *CgTyp-1* and *CgTyp-3* encoded putative proteins of 828 and 655 deduce amino acid respectively, which contained two copper-binding domains (Fig. 2B), displaying a high degree of similarity with other species tyrosinase or tyrosinase-like proteins. Signal peptide revealed that *CgTyp-1* possessed three low complexity domains which located in the 97–111, 209–219 and 445–453 residue regions, whereas *CgTyp-3* possessed a transmembrane region and a low complexity domain which located in the 5–22 and 547–558 residue regions, respectively.

The phylogenetic tree was constructed using the amino acid sequences to investigate the evolutionary relationships of tyrosinase and tyrosinase-like protein genes from different species. The tree was clustered into two large clades, in which one clade covered vertebrates including human, mouse, fish; the other clade was mollusk species, such as bivalvia and cephalopoda (Fig. 2C). What's more, *CgTyp-1* exhibited the closest relationship with *M. yessoensis*, and *CgTyp-3* was close to *C. virginica*.

3.2. Expression profiles of the CgTyp-1 and CgTyp-3 in tissues of C. gigas

Real–time PCR was conducted to identify two tyrosinase-like protein genes expression patterns in various tissues of the black shell *C. gigas*. Overall, different tissues varied in their tyrosinase-like protein genes expression. Two genes were significantly higher expressed in the mantle ($P < 0.05$), with lower levels or none in other tissues (Fig. 3A, D). The expression of *CgTyp-1* and *CgTyp-3* were recognized among different mantle regions in black shell oysters. Two genes were expressed at higher levels in the marginal mantle than central mantle whether on the left or right sides ($P < 0.05$) (Fig. 3B, E). Besides, a significantly high expression level of two genes was detected in the anterior areas of mantle compared with that in the posterior areas ($P < 0.05$). Nevertheless, the expression level of *CgTyp-1* in the anterior areas of the right mantle was significantly higher than that in the left mantle ($P < 0.05$) (Fig. 3B), while higher expression of the *CgTyp-3* was observed in the anterior areas of the left side ($P < 0.05$) (Fig. 3E).

The anterior side of left mantle was applied to compare expression profiles of shell color strains, due to the lower expression levels of tyrosinase-like protein genes found in the central mantle. It was clear that the expression levels of *CgTyp-1* and *CgTyp-3* in the black shell color oysters were significantly higher than that in the white shell color oysters ($P < 0.05$) (Fig. 3C, F).

3.3. Localization of the CgTyp-1 and CgTyp-3 mRNA in C. gigas mantle

To investigate whether *CgTyp-1* and *CgTyp-3* function in melanin synthesis or shell biosynthesis, tissue location of two genes transcripts was examined by ISH. *CgTyp-1* and *CgTyp-3* were specially expressed in the marginal mantle (Fig. 4). Notably, strong signals for *CgTyp-1* were detected in the outer surface of the outer fold either in the black (Fig. 4A, B) or white (Fig. 4C, D) shell color oysters based on the ISH analysis. Expression of *CgTyp-3* was different from the observation of *CgTyp-1*, it was found in the outer epithelium of the outer fold, but mainly distributed in the top of the outer fold (Fig. 4E-H).

3.4. RNAi-mediated CgTyp-1 and CgTyp-3 knockdown in C. gigas

RNA interference was carried out to further confirm the function of *CgTyp-1* and *CgTyp-3* in melanin synthesis, and qPCR was performed to evaluate the silencing effects. Increasing time of RNAi resulted in a change in mRNA expression of *CgTyp-1* and *CgTyp-3* in the mantle, while there was no trend of change for the two genes expression level in the
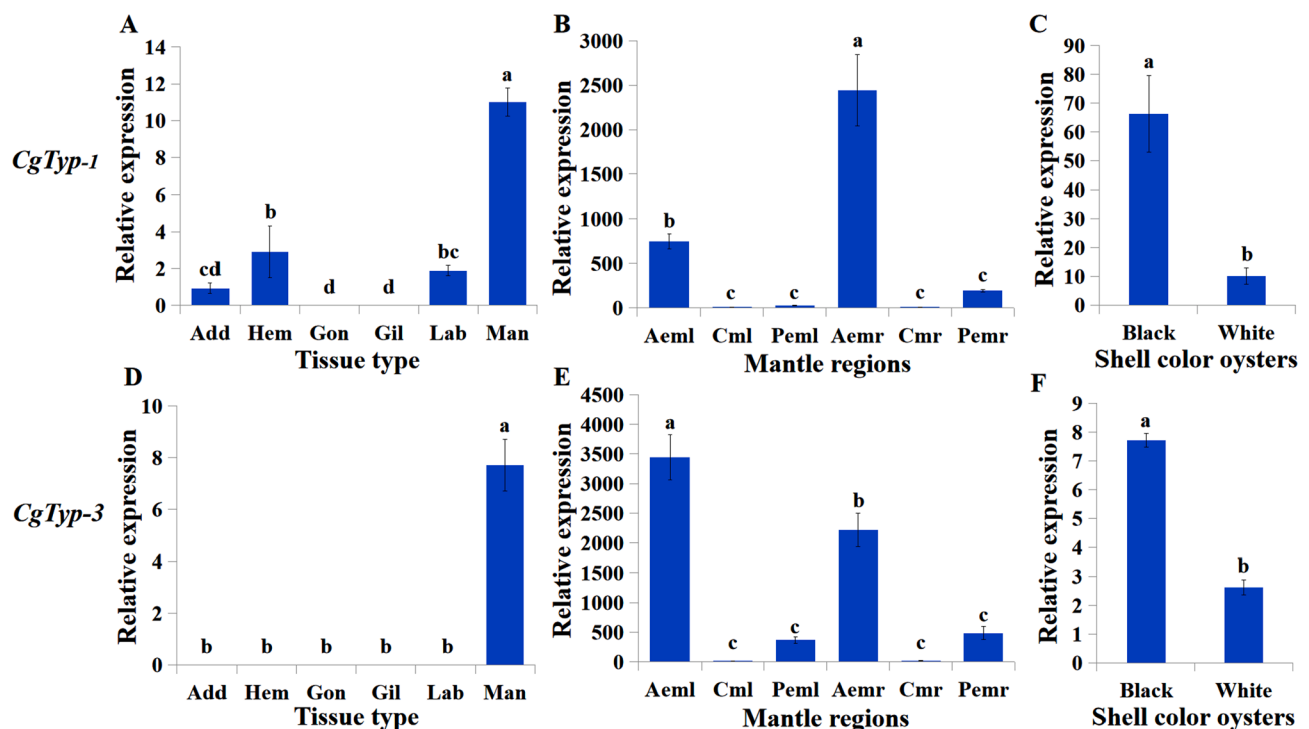

Fig. 3. The expression of *CgTyp-1* and *CgTyp-3*. Relative expression levels in tissue (A), mantle regions (B), and different shell color oysters (C) for *CgTyp-1*. Relative expression levels in tissue (A), mantle regions (B), and different shell color oysters (C) for *CgTyp-3*. Add, adductor muscle; Hem, hematocyte; Gon, gonad; Gil, gill; Lab, labial palp; Man, mantle; Aeml, anterior side of the left edge mantle; Cml, left central mantle; Peml, posterior side of the left edge mantle; Aemr, anterior side of the right edge mantle; Cmr, right central mantel; Pemr, posterior side of the right edge mantle; Black, black shell color oysters; White, white shell color oysters. The significant difference ($P < 0.05$) among various samples is indicated by the different lowercase letters.
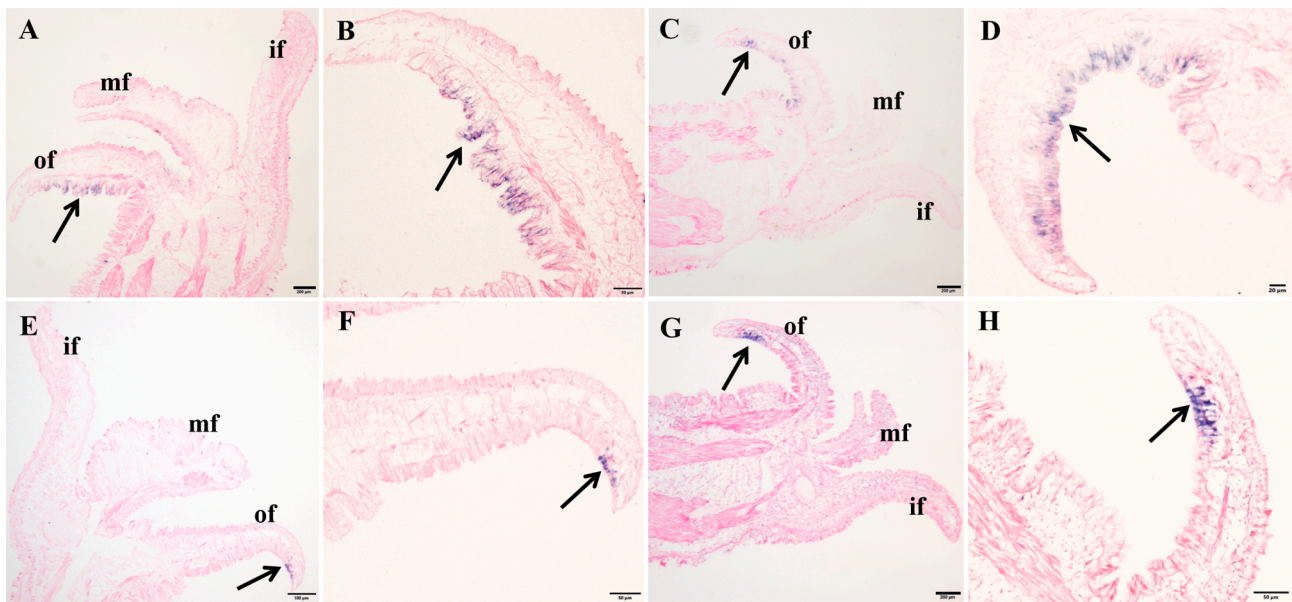
Fig. 4. *CgTyp-1* and *CgTyp-3* expression in the mantle of *C. gigas* by in situ hybridization. *CgTyp-1 is* found expressed in the black shell color oysters (A and B) and white shell color oysters (C and D). *CgTyp-3* is found expressed in the black shell color oysters (E and F) and white shell color oysters (G and H). Black arrows indicate the positive signals. of: outer fold; mf: middle fold; if: inner fold.

control group (Fig. 5A, D). Strikingly, the expression of *CgTyp-1* decreased significantly and then increased with the time of interference after injecting siRNA. The best interference effect was achieved at 12 h ($P < 0.01$), and the efficiency of RNAi reached 84.72% at this time point. The expression level of the RNAi group was also decreased compared with that of the control group until 48 h (Fig. 5A). In contrast, compared with the PBS-injected controls, *CgTyp-3* expression in siRNA-injected exhibited a trend decreasing with the time of interference, and highest interference effect appeared in 48 h ($P < 0.01$), which reached 71.58% (Fig. 5D).
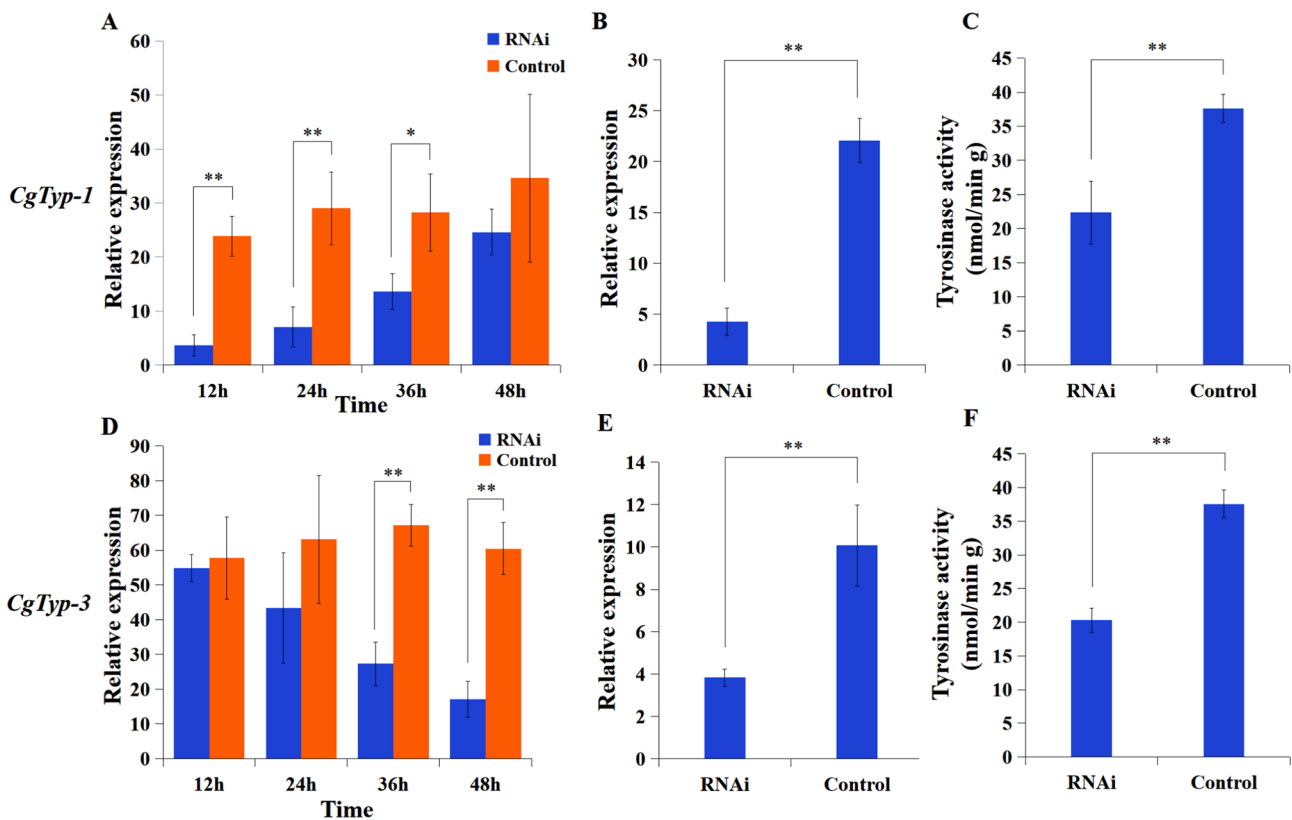

Fig. 5. The effect of genes silencing on genes expression and tyrosinase activity. Expression levels of *CgTyp-1* (A) and *CgTyp-3* (D) in the mantle at different time points after RNAi. Expression levels of *CgTyp-1* (B) and *CgTyp-3* (E) in the mantle at the 7th day after the injection. The tyrosinase activity of *CgTyp-1* group (C) and *CgTyp-3* group (F) in the mantle at the 7th day after the injection. 12 h, 24 h, 36 h and 48 h represent 12, 24, 36, and 48 h after the injection, respectively. Significant difference is indicated by * ($P < 0.05$) and highly significant difference is indicated by ** ($P < 0.01$).

In order to better reflect the interference effect, according to the pre-experimental results, we chose to inject into the experimental oysters at 48-h-long interval, and detected the expression at the 7th day after the siRNA injection. Apparently, qPCR analyses displayed that expression levels of *CgTyp-1* (Fig. 5B) and *CgTyp-3* (Fig. 5E) in RNAi groups were significantly lower than that in the control group ($P < 0.01$).

3.5. CgTyp-1 and CgTyp-3 silencing inhibited tyrosinase activity

The tyrosinase activity in mantles of the black shell colors after RNAi was shown in Fig. 5. The tyrosinase activity was obviously decreased either in siRNA *CgTyp-1* (Fig. 5C) or siRNA *CgTyp-3* (Fig. 5F) group compared to the control group ($P < 0.01$).

3.6. CgTyp-1 and CgTyp-3 silencing affected the distribution of melanosome of mantles

To further investigate the function of *CgTyp-1* and *CgTyp-3* in *C. gigas*, melanosomes in the outer surface of the outer fold of the mantle, known as unique organelles in melanin synthesis, was analyzed after RNA interference using a transmission electron microscopy. In the control group, a great deal of homogeneous melanosomes which contained melanin were distributed in epithelia of the mantle, and some were concentrated towards the apical microvillar surface near the lumen (black arrowheads) (Fig. 6A-D). Typically, granular endoplasmic reticulum (ger) and mitochondria (mi) were present in the peripheral region of melanosomes (Fig. 6B, D). In contrast to the control group, the number of high-melanization melanosomes within the outer fold were sharply reduced both in *CgTyp-1* siRNA and *CgTyp-3* siRNA groups. Besides, in *CgTyp-1* siRNA group, numerous melanosomes with non-pigmented and partially pigmented granules were abundantly found in the outer fold epithelium (Fig. 6E-H). Occasionally, melanosomes can also be observed in *CgTyp-3* siRNA group, but they were relatively less (Fig. 6K, L). Large number of non-pigmented melanosomes were found throughout the cells of epithelium (Fig. 6I-K), noticeably smaller numbers being found in the cells of the control group examined.

4. Discussion

The tyrosinase gene family has undergone a large expansion, leading to 12 paralogues and 24 duplicates genes in *C. gigas* (Aguilera et al., 2014). In this study, two tyrosinase-like genes (*CgTyp-1* and *CgTyp-3*) which belonged to the same tyrosinase gene family, were identified by the extensive analysis of data in the NCBI. Tyrosinase-like protein genes, as copper-binding proteins, possessed two conserved copper-binding sites, called as Cu (A) and Cu (B), each of which was coordinated by three conserved histidines, suggesting the potential homology. These sites were also observed in other copper-binding proteins, such as phenoloxidases, catecholoxidase, hemocyanin, and tyrosinases of various organisms (Decker and Tuczek, 2000; van Holde et al., 2001). These similar active sites indicated that tyrosinase-like protein genes had phenoloxidase function. Phylogenetic analysis further revealed close homology of the *C. gigas Typs* to the tyrosinase/tyrosinase-like in invertebrates, suggesting their ancestral evolutionary status.

Tyrosinases, which are characterized by oxygenase and oxidase activities, play a critical role in many biological activities, including insect cuticle sclerotization, pigmentation, formation of egg capsules, oxygen transport and wound healing (Andersen, 2010; Nagai et al., 2007; Cerenius et al., 2008; Bai et al., 1997). Tissue expression analysis indicated that *CgTyp-1* and *CgTyp-3* were predominantly expressed in the mantle. In bivalves, mantle have been implicated in biomineralization and pigment synthesis. That might explain why there were the highest expression of *CgTyp-1* and *CgTyp-3* in mantle. Besides, in the case of a bivalve the mantle is zootomically divided into two regions, namely
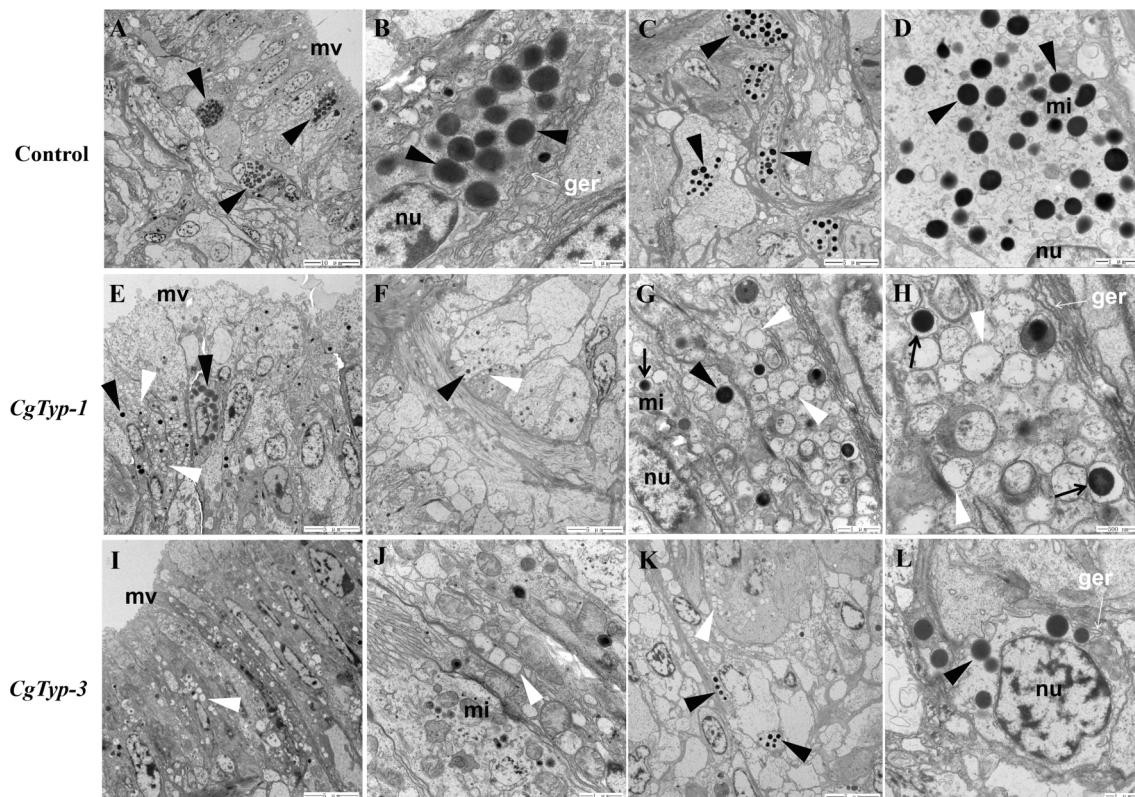

Fig. 6. Transmission electron microscopy of the outer fold of mantle epithelia in *C. gigas*. Ultrastructure of the outer fold of mantle epithelia are showed in the control group (A to D), *CgTyp-1* siRNA group (E to H) and *CgTyp-3* siRNA group (I to L). Black arrowheads indicate melanosomes. Black arrows indicate melanosomes with partially pigmented granules. White arrowheads indicate non-pigmented vesicles. mv, microvilli; nu, nuclei; mi, mitochondria; ger, granular endoplasmie retieulum.

marginal mantle and central mantle, in which the marginal mantle plays a role in the mineralization of prismatic shell layer and the central mantle is associated with the formation of nacreous shell layer (Aguilera et al., 2014). *CgTyp-1* and *CgTyp-3* genes were predominantly expressed in the marginal mantle, and hardly detectable in the central mantle, indicating that their expression were associated with the prismatic shell layer or periostracum construction. The ISH results further verified the expression of two genes that positive signals were only present in the marginal mantle but not in the central mantle.

Melanin synthesis in pigment cells is an enzymatic process that converts tyrosine to melanin (Yu et al., 2018). Tyrosinase is the first rate-limiting in melanogenesis which facilitates the formation of carboxy group-containing eumelanins in vertebrates and invertebrates (Camp et al., 2003). Research on tyrosinase/tyrosinase-like protein genes has concentrated on the function controlling the pigment formation in melanocytes (Vachtenheim and Borovanský, 2010). In molluscs, the mantle, as an evolutionarily homologous organ phenotypic diversity of mollusc shells, is thought to be responsible for the phenotypic diversity of mollusc shells (Sud et al., 2002; Jolly et al., 2004). Pigments produced by the mantle are incorporated into the shell along the growing edge and continually accumulated as new shell is added (Williams, 2017). White shell color oysters are supposed to be mainly the result of the absence of melanin biosynthesis or of synthesis of non- or partly functional melanin protein (Oetting and King, 1999). In the present study, two tyrosinase-like protein genes in mantles showed differential expression patterns between the black and white shell color oysters, implying that the two genes function in the mantle to regulate the shell pigmentation. On the other hand, it is generally believed that the prismatic layer of the shell arises from the mantle epithelial cells lining the outer surface of outer fold (Jabbour-Zahab et al., 1992). Based on the ISH analysis, *CgTyp-1* and *CgTyp-3* mRNA were found to be expressed in the outer epithelium of the outer fold, supporting the assumption that they contributed to the prismatic layer development. Moreover, the localization of tyrosinase proteins were observed in the prismatic shell layer, which is recognized as the pigmented zone in *P. fucata* (Nagai et al., 2007). Overall, our expression profile analyses suggested potentially diverse functions of the two tyrosinase-like protein genes in the oysters which are potentially involved in melanin biosynthesis and shell biomineralization. Similarly, *HcTyr* and *HcTyp-1* in *H. cumingii* were significantly expressed between purple and white mussel, and strong mRNA signals for *HcTyp-1* were expressed in the epithelium of the mantle pallial and periostracal groove revealing a potential role in periostracum and nacreous layer biomineralization, while *HcTyr* mRNA signals were found in the epithelium of the mantle pallial, revealing that *HcTyr* might involve in nacre calcification (Chen et al., 2017). Contrary to observations for *C. gigas*, OT47 gene (a homolog of tyrosinase related protein 1) from *P. margaritifera* was expressed significantly higher in full albino phenotypes than that in the half albino and black phenotypes, tend to suggest that the overexpression of this gene was correlated to overcompensate for a nonfunctional melanin protein (Lemer et al., 2015). In *P. fucata*, OT47 was primarily expressed in the middle fold of the mantle indicating its role in the periostracum development (Lemer et al., 2015).

To better understand the role of tyrosinase-like protein genes in melanin synthesis, RNAi was used to explore their function. The results showed that the gene was silenced in oysters by pericardial cavity injection of siRNA contained phenol red, which provided a new and effective way to study gene function at the individual level. Meanwhile, the expression levels of two genes were obviously attenuated after *CgTyp-1* and *CgTyp-3* interference, which indicated the high silencing efficiency of genes. Besides, the decreased tyrosinase activity observed from the two RNAi groups can be attributed to the silencing effects of the *CgTyp-1* siRNA and *CgTyp-3* siRNA. Indeed, some studies have presented evidence demonstrating that tyrosinase activity plays an important role in controlling mixed melanogenesis (Wakamatsu et al., 2021). When tyrosinase activity is significantly reduced, melanogenesis is suppressed to a stage where only the production of cysteinyldopa is apparent and

little to no pigment is produced (Lamoreux et al., 2001). These indicated *CgTyp-1* and *CgTyp-3* might be determinants of melanin synthesis in *C. gigas*. On the other hand, black color is mainly produced by melanocytes synthesizing melanin. Each melanocyte contains thousands of melanin-containing melanosomes, which is a specialized membrane-bound organelle that is involved in melanin synthesis, storage, and transportation (Marks and Seabra, 2001). Melanosomes are formed through a series of morphologically defined stages beginning with a membrane-bounded vesicle that is gradually filled with electron-dense melanin (Aspengren et al., 2008). It was reported that melanocytic activity in each melanocyte and the size and maturation of the melanosomes can cause skin differences (Miyamura et al., 2007). In this study, there were numerous, mature, large melanosomes which characterized by ellipsoidal and intensely melanotic within the outer fold epithelium in the control group, while the melanosomes both in *CgTyp-1* siRNA and *CgTyp-3* siRNA groups proved to be smaller and less dense, reflecting an impaired melanogenesis in RNAi groups. Generally, tyrosinase and tyrosinase-related protein 1 are synthesized on ribosomes and are transported through the endoplasmic reticulum and Golgi apparatus. Then these melanogenic enzymes are sorted from the trans-Golgi network to early melanosomes by secretory vesicles, after that they are localized in the limiting membrane of these organelles, where the synthesis of melanin usually begins (Costin et al., 2003). Based on these, it was speculated that the tyrosinase processing and trafficking were disrupted before delivery to early melanosomes after tyrosinase-like protein genes silencing, thus explaining the reduced melanosomes seen in RNAi groups melanocytes. Taken together, knockdown *CgTyp-1* and *CgTyp-3* greatly reduce tyrosinase catalytic activity and melanin production indicating the two genes have large potential in the synthesis of melanin pigments in *C. gigas*. Similarly, knockdown *D. rerio Tyrp1* led to the production of brown instead of black eumelanin accompanied by severe melanosome defects, indicating *Tyrp1* could function in the black eumelanin formation (Braasch et al., 2009). In the absence of *PpTyr* in *P. penguin*, the content of PDCA and PTCA (eumelanin markers) was sharply decreased, indicating its role in melanin biosynthesis (Yu et al., 2018).

In conclusion, two tyrosinase-like protein genes were identified in the Pacific oyster, sequence and structural characterization of the genes confirmed their identities; phylogenetic analysis revealed the molecular evolution of *Typs*. Expression patterns of *CgTyp-3* and *CgTyp-3* of oysters suggested the potential ability of two genes in the shell biosynthesis and pigmentation. The altered tyrosinase activity and melanosomes after the two genes silencing further supported their biological functions in the synthesis of melanin pigments. The work enables deeper insight into shell pigmentation regulation mechanisms in the Pacific oyster.

Declaration of Competing Interest

The authors declare that they have no known competing financial interests or personal relationships that could have appeared to influence the work reported in this paper.

Data availability

Data will be made available on request.

Acknowledgements

References

Aguilera, F., McDougall, C., Degnan, B.M., 2014. Evolution of the tyrosinase gene family in bivalve molluscs: independent expansion of the mantle gene repertoire. Acta Biomater. 10, 3855–3865.

Alfnes, F., Guttormsen, A.G., Steine, G., Kolstad, K., 2006. Consumers' willingness to pay for the color of salmon: a choice experiment with real economic incentives. Am. J. Agric. Econ. 88, 1050–1061.

Andersen, S.O., 2010. Insect cuticular sclerotization: a review. Insect Biochem. Mol. Biol. 40, 166–178.

Aspengren, S., Hedberg, D., Sköld, H.N., Wallin, M., 2008. Chapter 6 new insights in melanosome transport in vertebrate pigment cells. Int. Rev. Cel. Mol. Bio. 272, 245–302.

Bai, G., Brown, J.F., Watson, C., Yoshino, T.P., 1997. Isolation and Characterization of Phenoloxidase from Egg Masses of the Gastropod Mollusc, *Biomphalaria glabrata*. Comp. Biochem. Physiol. B Comp. Biochem. 118, 463–469.

Bergamonti, L., Bersani, D., Mantovan, S., Lottici, P.P., 2013. Micro-Raman investigation of pigments and carbonate phases in corals and molluscan shells. Eur. J. Haematol. 25, 845–853.

Boutros, M., Kiger, A.A., Armknecht, S., Kerr, K., Hild, M., Koch, B., Haas, S.A., Consortium, H.F.A., Paro, R., Perrimon, N., 2004. Genome-wide RNAi analysis of growth and viability in Drosophila cells. Science 303, 832–835.

Braasch, I., Liedtke, D., Volff, J.N., Schartl, M., 2009. Pigmentary function and evolution of *tyrp1* gene duplicates in fish. Pigm. Cell Melanoma R. 22, 839–850.

Brake, J., Evans, F., Langdon, C., 2004. Evidence for genetic control of pigmentation of shell and mantle edge in selected families of Pacific oysters, *Crassostrea gigas*. Aquaculture 229, 89–98.

Cai, Z., Wu, J., Chen, L., Guo, W., Li, J., Wang, J., Zhang, Q., 2011. Purification and characterisation of aquamarine blue pigment from the shells of abalone (*Haliotis discus hannai* Ino). Food Chem. 128, 129–133.

Camp, E., Badhwar, P., Mann, G.J., Lardelli, M., 2003. Expression analysis of a tyrosinase promoter sequence in zebrafish. Pigm. Cell Res. 16, 117–126.

Cerenius, L., Lee, B.L., Söderhäll, K., 2008. The proPO-system: pros and cons for its role in invertebrate immunity. Trends Immunol. 29, 263–271.

Chen, D.S., Chan, K.M., 2012. Identification of hepatic copper-binding proteins from tilapia by column chromatography with proteomic approaches. Metallomics 4, 820–834.

Chen, X., Liu, X., Bai, Z., Zhao, L., Li, J., 2017. HcTyr and HcTyp-1 of *Hyriopsis cumingii*, novel tyrosinase and tyrosinase-related protein genes involved in nacre color formation. Comp. Biochem. Physiol. B Biochem. Mol. Biol. 204, 1–8.

Costin, G.E., Valencia, J.C., Vieira, W.D., Lamoreux, M.L., Hearing, V.J., 2003. Tyrosinase processing and intracellular trafficking is disrupted in mouse primary melanocytes carrying the *underwhite* (uw) mutation. A model for oculocutaneous albinism (OCA) type 4. J. Cell Sci. 116, 3203–3212.

Cullen, L.M., Arndt, G.M., 2005. Genome-wide screening for gene function using RNAi in mammalian cells. Immunol. Cell Biol. 83, 217–223.

Decker, H., Tuczek, F., 2000. Tyrosinase/catecholoxidase activity of hemocyanins: structural basis and molecular mechanism. Trends Biochem. Sci. 25, 392–397.

Derby, C.D., 2014. Cephalopod ink: production, chemistry, functions and applications. Mar. Drugs 12, 2700–2730.

Feng, D., Li, Q., Yu, H., 2019. RNA interference by ingested dsRNA-expressing bacteria to study shell biosynthesis and pigmentation in *Crassostrea gigas*. Mar. Biotechnol. 21, 526–536.

Feng, D., Li, Q., Yu, H., Kong, L., Du, S., 2017. Identification of conserved proteins from diverse shell matrix proteome in *Crassostrea gigas*: Characterization of genetic bases regulating shell formation. Sci. Rep. 7, 45754.

Hoekstra, H.E., 2006. Genetics, development and evolution of adaptive pigmentation in vertebrates. Heredity 97, 222–234.

Jabbour-Zahab, R., Chagot, D., Blanc, F., Grizel, H., 1992. Mantle histology, histochemistry and ultrastructure of the pearl oyster *Pinctada margaritifera* (L.). Aquat. Living Res. 5, 287–298.

Jiang, K., Jiang, L., Nie, H., Huo, Z., Yan, X., 2020. Molecular cloning and expression analysis of tyrosinases (*tyr*) in four shell-color strains of Manila clam *Ruditapes philippinarum*. PeerJ 8, e8641.

Johansson, M.W., Soderhall, K., 1996. The prophenoloxidase activating system and associated proteins in invertebrates. Invertebrate Immunology, Progress in Molecular and Subcellular Biology, Vol. 15, Springer-Verlag, Berlin Heidelberg, pp. 46–66.

Jolly, C., Berland, S., Milet, C., Borzeix, S., Lopez, E., Doumenc, D., 2004. Zonal localization of shell matrix proteins in mantle of *Haliotis tuberculata* (Mollusca, Gastropoda). Mar. Biotechnol. 6, 541–551.

Kobayashi, T., Kawahara, I., Hasakura, O., Kijima, A., 2004. Genetic control of bluish shell color variation in the Pacific abalone *Haliotis discus* hannai. J. Shellfish Res. 23, 1153–1156.

Lamoreux, M.L., Wakamatsu, K., Ito, S., 2001. Interaction of major coat color gene functions in mice as studied by chemical analysis of eumelanin and pheomelanin. Pigm. Cell Res. 14, 23–31.

Lecompte, O., Madec, L., Daguzan, J., 1998. Temperature and phenotypic plasticity in the shell colour and banding of the land snail *Helix aspersa*. Comptes Rendus de l'Academie des Sciences, Series III, Sciences de la vie 8, 649–654.

Lemer, S., Saulnier, D., Gueguen, Y., Planes, S., 2015. Identification of genes associated with shell color in the black-lipped pearl oyster, *Pinctada Margaritifera*. BMC Genom. 16, 568.

Letunic, I., Doerks, T., Bork, P., 2015. SMART: recent updates, new developments and status in 2015. Nucleic Acids Res. 43, D257–D260.

Liu, X., Wu, F., Zhao, H., Zang, G., Guo, X., 2009. A novel shell color variant of the Pacific abalone *Haliotis discus hannai* Ino subject to genetic control and dietary influence. J. Shellfish Res. 28, 419–424.

Liu, Y., Li, L., Huang, B., Wang, W., Zhang, G., 2019. RNAi based transcriptome suggests genes potentially regulated by HSF1 in the Pacific oyster *Crassostrea gigas* under thermal stress. BMC Genom. 20, 639.

Marks, M.S., Seabra, M.C., 2001. The melanosome: membrane dynamics in black and white. Nat. Rev. Mol. Cell Bio. 2, 738–748.

Miyamura, Y., Coelho, S.G., Wolber, R., Miller, S.A., Wakamatsu, K., Zmudzka, B.Z., Ito, S., Smuda, C., Passeron, T., Choi, W., Batzer, J., Yamaguchi, Y., 2007. Regulation of human skin pigmentation and responses to ultraviolet radiation. Pigm. Cell Res. 20, 2–13.

Nagai, K., Yano, M., Morimoto, K., Miyamoto, H., 2007. Tyrosinase localization in mollusc shells. Comp. Biochem. Physiol. B Biochem. Mol. Biol. 146, 207–214.

Nell, J.A., 2001. The history of oyster farming in Australia. Mar. Fish. Rev. 63, 14–25.

Oetting, W.S., King, R.A., 1999. Molecular basis of albinism: Mutations and polymorphisms of pigmentation genes associated with albinism. Hum. Mutat. 13, 99–115.

Palumbo, A., 2003. Melanogenesis in the Ink Gland of *Sepia officinalis*. Pigm. Cell Res. 16, 517–522.

Sokolova, I.M., Berger, V.J., 2000. Physiological variation related to shell colour polymorphism in White Sea *Littorina saxatilis*. J. Exp. Mar. Biol. Ecol. 245, 1–23.

Sud, D., Poncet, J., Saihi, A., Lebel, J., Doumenc, D., Boucaud-Camou, E., 2002. A cytological study of the mantle edge of *Haliotis tuberculata* L. (Mollusca, Gastropoda) in relation to shell structure. J. Shellfish Res. 21, 201–210.

Vachtenheim, J., Borovanský, J., 2010. "Transcription physiology" of pigment formation in melanocytes: central role of MITF: Transcription of pigmentation-related genes. Exp. Dermatol. 19, 617–627.

van Holde, K.E., Miller, K.I., Decker, H., 2001. Hemocyanins and invertebrate evolution. J. Biol. Chem. 276, 15563–15566.

Wakamatsu, K., Zippin, J.H., Ito, S., 2021. Chemical and biochemical control of skin pigmentation with special emphasis on mixed melanogenesis. Pigm. Cell Melano. Res. 34, 730–747.

Whiteley, D.A.A., Owen, D.F., Smith, D.A.S., 1997. Massive polymorphism and natural selection in *Donacilla cornea* (Poli, 1791) (Bivalvia: Mesodesmatidae). Biol. J. Linn. Soc. 62, 475–494.

Williams, S.T., 2017. Molluscan shell colour. Biol. Rev. 92, 1039–1058.

Xu, R., Li, Q., Yu, H., Kong, L., 2018. Oocyte maturation and origin of the germline as revealed by the expression of Nanos-like in the Pacific oyster *Crassostrea gigas*. Gene 663, 41–50.

Yao, H., Cui, B., Li, X., Lin, Z., Dong, Y., 2020. Characteristics of a novel tyrosinase gene involved in the formation of shell color in Hard clam *Meretrix meretrix*. J. Ocean Univ. China 19, 183–190.

Yu, F., Pan, Z., Qu, B., Yu, X., Xu, K., Deng, Y., Liang, F., 2018. Identification of a tyrosinase gene and its functional analysis in melanin synthesis of *Pteria penguin*. Gene 656, 1–8.

Zhu, Y., Li, Q., Yu, H., Kong, L., 2018. Biochemical composition and nutritional value of different shell color strains of Pacific oyster *Crassostrea gigas*. J. Ocean Univ. China 17, 897–904.

Zhu, Y., Li, Q., Yu, H., Liu, S., Kong, L., 2021. Shell biosynthesis and pigmentation as revealed by the expression of tyrosinase and tyrosinase-like protein genes in Pacific oyster (*Crassostrea gigas*) with different shell colors. Mar. Biotechnol. 23, 777–789.